



**HAL**  
open science

# Analysis of particle trajectory in nanosecond pulsed DBD-ESP using time-resolved particle image velocimetry

Noureddine Zouzou, Arthur Claude Aba'a Ndong, Eric Moreau

► **To cite this version:**

Noureddine Zouzou, Arthur Claude Aba'a Ndong, Eric Moreau. Analysis of particle trajectory in nanosecond pulsed DBD-ESP using time-resolved particle image velocimetry. XIV International Conference on Electrostatic Precipitation, ICESP'2016, Sep 2016, Wroclaw, Poland. hal-04489655

**HAL Id: hal-04489655**

**<https://hal.science/hal-04489655>**

Submitted on 5 Mar 2024

**HAL** is a multi-disciplinary open access archive for the deposit and dissemination of scientific research documents, whether they are published or not. The documents may come from teaching and research institutions in France or abroad, or from public or private research centers.

L'archive ouverte pluridisciplinaire **HAL**, est destinée au dépôt et à la diffusion de documents scientifiques de niveau recherche, publiés ou non, émanant des établissements d'enseignement et de recherche français ou étrangers, des laboratoires publics ou privés.

# Analysis of particle trajectory in nanosecond pulsed DBD-ESP using time-resolved particle image velocimetry

N. Zouzou, A. C. Aba'a Ndong, E. Moreau

*Institut Pprime, UPR 3346, CNRS – Université de Poitiers – ISAE-ENSMA*

*F86962, Futuroscope Chasseneuil Cedex, France*

Corresponding author: [noureddine.zouzou@univ-poitiers.fr](mailto:noureddine.zouzou@univ-poitiers.fr)

Keywords: Nanosecond pulsed DBD, electrohydrodynamic flow, PIV, electrostatic precipitators

## Abstract

In this paper, the interaction between nanosecond pulsed dielectric barrier discharge and submicron particles is investigated experimentally using particle image velocimetry technique in a wire-to-plane electrostatic precipitator. The induced electrohydrodynamic phenomena have been studied by using time-resolved measurements for both positive and negative polarities of the nanosecond pulsed high voltage. The main results indicate that the velocity of particles is considerably affected by the negative discharges related to the negative transition of the voltage pulse, whatever the polarity. This is probably due to the contribution of the electric wind that could affect both the trajectories of charged and uncharged particles.

## 1. Introduction

In the past decade, several studies demonstrate the great potential of dielectric barrier discharge based electrostatic precipitators (DBD-ESPs) energized by a low frequency ac high voltage for the collection of submicrometer particles [1-6]. The frequencies range from a few Hz to several kHz, for voltages up to 30 kV. In most cases, the power supply system includes a high voltage linear amplifier with moderate slew rate (less than 1 kV/ $\mu$ s). However, only few studies deal with the use of nanosecond pulsed voltage (rise and fall times in the range of a few ns) for the electrostatic precipitation of particles [7].

The goal of the work presented here is to investigate how the DBD interacts with submicron particles during and after the application of nanosecond pulsed high voltages. Thus, time-resolved particle image velocimetry (TR-PIV) technique is used to measure the instantaneous velocity fields for both positive and negative polarities of the applied voltage.

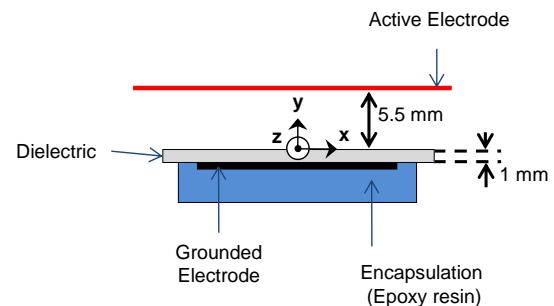
In the first part of this paper, the experimental setup is described. Then, results concerning the discharge characteristics and particle velocity fields are discussed. Finally, conclusions are summarized.

## 2. Experimental setup

### 2.1. Geometric configuration

The investigation is carried out with a wire-to-plane geometry shown in Fig. 1. The configuration is composed of two electrodes separated by a dielectric barrier (Pyrex, 1 mm thick, 200 mm in length, and 100 mm in width). The active electrode consists of a nickel wire (0.2 mm in diameter). The plane electrode (aluminum tape, 20 mm in length, 20 mm in width and 70  $\mu$ m thick) is placed on the lower side of the dielectric barrier and encapsulated. The air gap is fixed at 5.5 mm in all experiments.

Side view



Top view

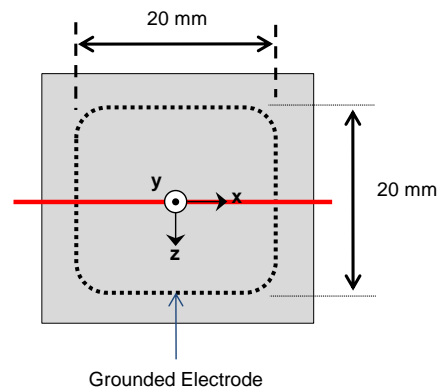


Fig. 1. Top and side views of the wire-to-plane geometry.

## 2.2. Electrical devices

The high voltage power supply is composed with an HV solid-state pulser (DEI, model PVX-4110), a DC power supply (Matsuda, model 10P30) and a digital pulse generator (Stanford, model DG645). The power supply can provide high voltage pulses up to  $\pm 10$  kV, whose rise and decay times are about 50 ns. By connecting two pulsers (arranged in series-opposition), the potential difference between active and collecting electrodes can reach  $\pm 20$  kV.

The total current is measured using a fast current transformer (Bergoz, model CT-D1.0) and the potential difference across the ESP is measured with a high voltage probe (LeCroy, model PPE20kV).

The digital pulse generator is also used as a synchronizer for triggering the TR-PIV system with the electrical signal supplied to the ESP.

More details about the experimental setup can be found in [8].

## 2.3. Particle tracking using time-resolved PIV

Submicron particles, with a mean size of about 0.28  $\mu\text{m}$ , are generated from incense burning and introduced into a closed box made of glass (80 cm  $\times$  40 cm  $\times$  30 cm) in order to examine the velocity of particles induced by pulsed discharges in the inter-electrode gap.

The particle velocity fields in the gap are analyzed experimentally using a time-resolved PIV device as illustrated in Fig. 2. This system is manufactured by LaVision. The PIV system uses a dual-head high-speed laser system (model Quantonix, Darwin-527-30-MM-PIV, type Nd-YLF, 527 nm wavelength) coupled to a 10 bit high-speed camera (Model Photron Fastcam SA1.1-675-M3, resolution of 1024 $\times$ 1024 pixels<sup>2</sup>). The acquisition rate is set to 10 kHz, allowing a good analysis of particle flow dynamics.

All the experiments are carried out at atmospheric pressure and room temperature.

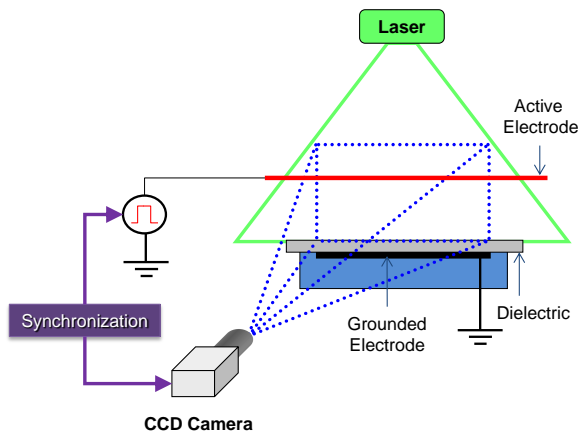


Fig. 2. Schematic illustration of the time-resolved particle image velocimetry setup.

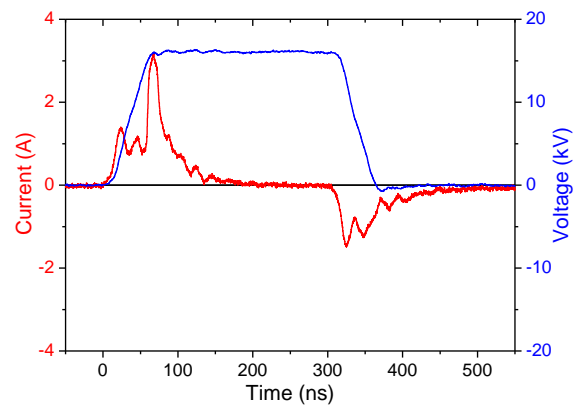
## 3. Experimental results

### 3.1. Current waveforms

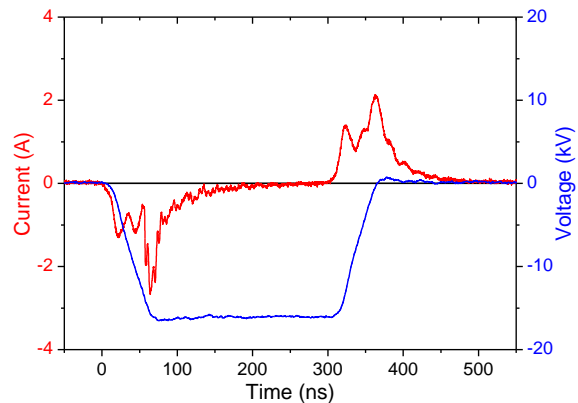
The typical waveforms of the nanosecond pulsed voltage and the associated current are shown in Fig. 2 for both positive and negative polarities. The ESP is supplied with a voltage pulse of  $\pm 16$  kV for a pulse width of about 300 ns.

The current waveform shows two peaks well resolved during rise and fall times of the voltage pulse, whatever the polarity. The first current peak is due to the deposition of electric charges (with the same polarity than the active electrode) produced by the discharge initiated close to the wire where the electric field is sufficiently intense. During the voltage plateau, the current level decreases rapidly and the discharge is then in its silent period.

When the potential difference between the wire and the charged dielectric surface is one more time sufficient, a new discharge propagates in the gap; this is the second discharge which takes place during the second transition of the voltage. Hence, the second current peak appears.



(a)



(b)

Fig. 3. Typical waveforms of the applied voltage and the discharge current for (a) positive polarity, and (b) negative polarity. Conditions: voltage =  $\pm 16$  kV, frequency = 0.5 Hz and pulse width = 300 ns.

The shape of the current peaks is nearly similar; however the discharge regimes associated to each one are completely different. In fact, the positive rise of the voltage pulse favors the formation of a streamer discharge, whereas the negative decay is associated with a corona-glow regime [7].

### 3.2. Particle Trajectories

In order to analyze particle trajectories in the gap, several sequences of 1300 pairs of images are recorded using high-speed camera with frame rates of 10 kHz for each pulse polarity. They correspond to 13 complete cycles of the applied voltage at the frequency of 100 Hz (1 period = 10 ms). Thus, the time required for a complete acquisition is about 130 ms. In this paper, we will present only some representative results corresponding to the first period. Fig. 4 shows a schematic illustration of the analyzed moments in the case on applied voltage of  $\pm 18$  kV and a frequency of 100 Hz with duty cycle of 25% (pulse width = 2.5 ms).

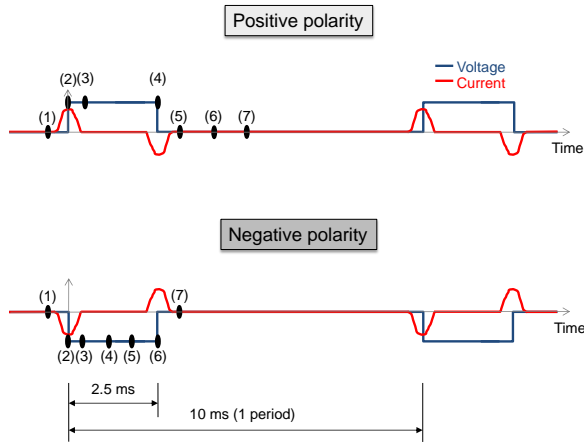


Fig. 4. Schematic illustration of the representative times of the analyzed sequence for both positive and negative polarities (duty cycle = 25%).

#### 3.2.1. EHD flow with positive polarity

Fig. 5 shows the typical grayscale images and velocity vector fields measured using time-resolved PIV in the case of positive polarity. The frames correspond to the representative times designated in the previous section.

For each velocity fields figure, the arrows indicate the module and the direction of the velocity in the  $xy$  plane, while the color bar shows the module of this velocity in the same plane.

For  $t < 2.5$  ms, one cannot observe a significant movement of particles in the gap even if a positive discharge (streamers) occurs during the rise time of positive voltage pulse from 0 to +18 kV. The signature of streamers is clearly visible near the active electrode on the grayscale image Fig. 5 (b), while the corresponding velocity fields (Fig. 5 (i)) show that

there is practically no drift of particles in the inter-electrode space. This means that the positive discharge characterized by streamer-like regime does not allow the electrostatic precipitation of particles in the case of nanosecond pulsed voltage.

For  $t \geq 2.5$  ms, the grayscale images and velocity fields are considerably affected due the occurrence of the negative discharge (glow-like regime) during the decay time of the positive pulse from +18 kV to 0 kV. For instance, one can observe a movement of particles near the dielectric barrier surface in Fig. 5 (k) at the end of the negative discharge. Thereafter, from  $t = 2.5$  to 4.3 ms, when the applied voltage returns to zero, the particles move from the active electrode toward the dielectric surface (Fig. 5 (e) – (g)), leaving in their wake areas at which the concentration of particle is low. The corresponding velocity field at these moments show localized particle acceleration (Fig. 5 (l) – (n)). In particular, the signature of at least 8 vortices is observed in the gap.

Several reasons could explain the strong EHD phenomena observed at the end of the voltage pulse, in particular: electric wind and electrostatic precipitation effects. However, if we take into account the particle trajectories in a vortex-induced flow, the effect of the electric wind on weakly charged particles appears to be significant. Furthermore, the electrostatic precipitation of negatively charged particles is possible during the phase when the applied voltage is close to zero. This is due to the electric field induced by the positive space charge deposited far from the inter-electrode space after streamers propagation.

#### 3.2.2. EHD flow with negative polarity

The typical grayscale images and the velocity vector fields obtained in the case of negative nanosecond pulsed voltage are shown in Fig. 6.

Before the application of the negative voltage pulse on the active electrode, the PIV system did not detects any significant movement of particles (Fig. 6 (a) and (h)). However, the negative discharge, initiated during the decay time of the voltage pulse from 0 to -18 kV, generates an important displacement of particles (Fig. 6 (b) and (i)), as in positive polarity. The consequences of the negative discharge persist until the end of the period.

As indicated by the grayscale images (Fig. 6 (c) and (j)), several areas with low particle concentration appear and develop from the active electrode toward the dielectric wall. The corresponding velocity fields show particle acceleration and the occurrence of several vortex (Fig. 6 (j) and (n)).

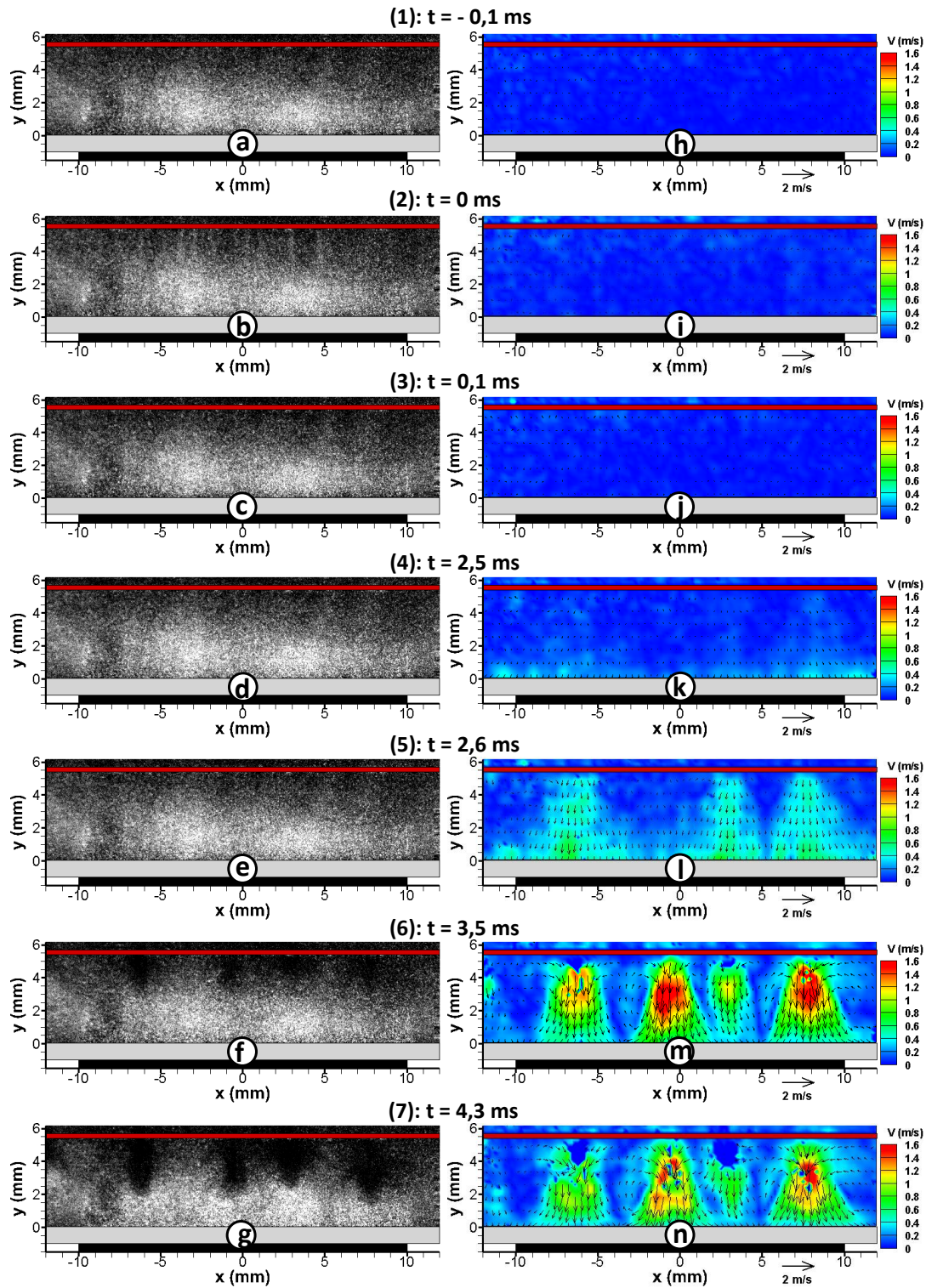


Fig. 5. Typical EHD phenomena observed during the positive voltage pulse. Conditions: voltage = + 18 kV, frequency = 100 Hz, pulse width = 10 ms (duty cycle = 25%).

The positive discharge, which occurs during the rise time of the negative pulse from -18 kV to 0 kV ( $t=2.5$  ms), does not appear to show a significant effect on the EHD flow induced by the negative discharge. Nevertheless, one can note the return of some particles towards the active electrode and the intensification of

the  $x$ -component of the velocity near the dielectric surface.

These results confirm the observations made in the previous section. Thus, the particle movements in the gap are mainly due to negative discharge generated during the decay time of the voltage pulse, whatever the polarity.

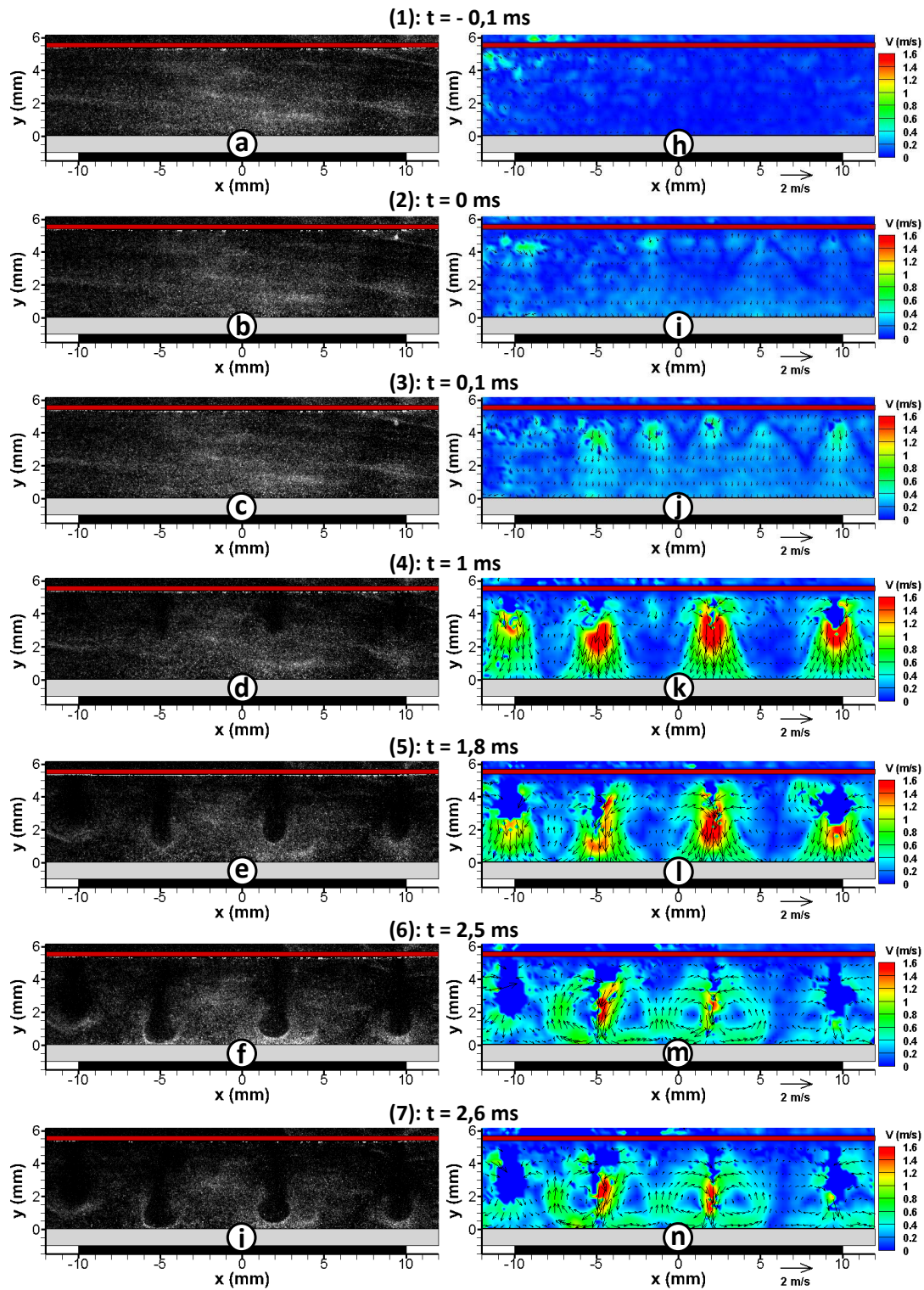


Fig. 6. Typical EHD phenomena observed during negative voltage pulse. Conditions: voltage = - 18 kV, frequency = 100 Hz, pulse width = 10 ms (duty cycle = 25%).

#### 4. Conclusion

In this paper, the interaction between nanosecond pulsed dielectric barrier discharge and submicron particles is investigated experimentally using particle image velocimetry technique in a wire-to-plane geometry. In particular, particle instantaneous velocity

fields have been analyzed for both positive and negative polarities of the nanosecond pulsed high voltage.

The main results of this experimental study are as follows.

(1) Whatever the voltage polarity, the EHD phenomena are observed after the negative discharge occurring during the decay time of the voltage pulse, while the positive discharge initiated during the rise time of the voltage pulse has no significant effect on particles movement.

(2) The movement of particle is probably due to the contribution of the electric wind that could affect both the trajectories of charged and uncharged particles.

(3) Electrostatic precipitation of particle is possible at the end of the positive pulse, even when the applied voltage returns to zero. This is due to the electric field induced by the positive space charge deposited far from the inter-electrode space after streamer propagation.

### References

- [1] Dramane B., Zouzou N., Moreau E., Touchard G., *Journal of Electrostatics*, (2009) vol. 67, pp. 117–122.
- [2] Dramane B., Zouzou N., Moreau E., Touchard G., *IEEE Transactions on Dielectrics and Electrical Insulation*, (2009), vol. 16, pp. 343–351.
- [3] Zouzou N., Dramane B., Moreau E., Touchard G., *IEEE Transactions on Industry Applications*, (2011), vol. 47, pp. 336-343.
- [4] Gouri R., Zouzou N., Tilmatine A., Moreau E., Dascalescu L., *Journal of Physics D: Applied Physics*, (2011), vol. 44, pp. 1-8.
- [5] Gouri R., Zouzou N., Tilmatine A., Dascalescu L., *Journal of Electrostatics*, (2013), vol. 71, pp. 240-245.
- [6] Gouri R., Zouzou N., Tilmatine A., Dascalescu L., *IEEE Transactions on Dielectrics and Electrical Insulation*, (2013), vol. 20, pp. 1540-1546.
- [7] Aba'a Ndong A. C., Zouzou N., Moreau E., in *Proc. International Symposium on Electrohydrodynamics ISEHD'2014*, Okinawa, Japan, June 23-25 (2014).
- [8] Aba'a Ndong A. C., Zouzou N., Benard N., Moreau E., *Journal of Electrostatics* (2013), vol. 71, pp. 246-253.